

EXPERIMENTAL CHARACTERIZATION OF AN INNOVATIVE COPPER-MARAGING STEEL METAL-MATRIX-COMPOSITE MATERIAL FOR A LIQUID ROCKET ENGINE THRUST CHAMBERS BY L-PBF

Original

EXPERIMENTAL CHARACTERIZATION OF AN INNOVATIVE COPPER-MARAGING STEEL METAL-MATRIX-COMPOSITE MATERIAL FOR A LIQUID ROCKET ENGINE THRUST CHAMBERS BY L-PBF ADDITIVE MANUFACTURING / Crachi, M; Sesana, R; Pizzarelli, M; Delprete, C; Borrelli, D; Sicignano, N. - ELETTRONICO. - (2023), pp. 1081-1090. (Intervento presentato al convegno 20th International Conference on Experimental Mechanics tenutosi a Oporto nel 2-7 July 2023).

Availability:

This version is available at: 11583/2980316 since: 2023-07-15T16:34:23Z

Publisher:

INEGI-FEUP

Published

DOI:

Terms of use:

This article is made available under terms and conditions as specified in the corresponding bibliographic description in the repository

Publisher copyright

(Article begins on next page)

EXPERIMENTAL CHARACTERIZATION OF AN INNOVATIVE COPPER-MARAGING STEEL METAL-MATRIX-COMPOSITE MATERIAL FOR A LIQUID ROCKET ENGINE THRUST CHAMBERS BY L-PBF ADDITIVE MANUFACTURING

Matteo Crachi^{1(*)}, Raffaella Sesana¹, Marco Pizzarelli², Cristiana Delprete¹, Domenico Borrelli³, Nicola Sicignano³

¹DIMEAS, Department of Mechanical and Aerospace Engineering, Politecnico di Torino, Torino, Italy

²Italian Space Agency (ASI), Roma, Italy

³Sophia High Tech, Somma Vesuviana 80049, Via Malatesta 30 A, Italy

(*)Email: matteo.crachi@polito.it

ABSTRACT

Thrust chamber of high performance bi-propellant liquid rocket engines is a critical component of the launch vehicles. The requirement of reducing the temperature of the walls exposed to the hot gas can be met with high-thermal conductivity copper alloys while the mechanical stiffness is achieved by using high strength steel or nickel alloys. Because the stress–strain behavior of a regeneratively cooled thrust chamber is directly correlated with its temperature behavior, it is of primary importance to select an adequate alloy. A new copper-steel metal matrix composite, processed by L-PBF additive manufacturing, is proposed. A patented innovative additive manufacturing powders mixing process is used. A thermal, mechanical and fatigue characterization of the new composite was performed. A new time dependent material behavior has been pointed out. It is a “local hill softening-hardening phenomenon”, which is a time dependent activated damage which occurs during cycling and creep tests at high temperature.

Keywords: metal matrix composite (MMC), additive manufacturing, liquid rocket engine, low cycle fatigue, copper, maraging steel, 174PH, powder mix.

INTRODUCTION

Space has become an important means to achieve goals in key policy areas including the environment, security, economic development, mobility and resource management [1]. The Space Economy includes public and private actors involved in development, provision and use of space products and services such as research and development, production and use of space infrastructure in order to make applications viable, as well as develop related research. It follows that the Space Economy goes beyond the space sector in the strict sense but extends its technological and scientific results to more areas of community life.

The present research origins in the context of the New Space Economy. Thanks to the capital invested in the space sector, the incentive to develop new technologies in the space sector has, for example, led to the Powder Mixing System developed and qualified by Sophia High tech s.r.l. This system is used in the present study to realize the starting customized powder mix for the SLM printing tasks, investigated in this work. This study provides a first thermomechanical characterization of the metal matrix composite object of this work in order to understand if it can be proposed for the design of reusable rocket engines. The idea is to obtain, with respect to typical requirements and operating conditions of this component, good thermal conductivity

with excellent tensile strength at high temperatures and cyclic behavior in the plastic range which does not develop the problems of deformation and crack nucleation. These properties were identified from pure copper and a common stainless steel in the world of additive manufacturing: 17-4 PH maraging steel.

The experimental activities began with the POWMIX powder mixer, developed and patented by Sophia High Tech: it is a new technology developed to mix two or more powder materials for additive manufacturing with an inert gas as mixing vehicle. Due to possible density and uniformity instabilities during mixing, an acoustic field is used in this system to break electrostatic forces and ensure a stochastic distribution of the mixed powder from the starting powders on the press platform. The scheme of the system is reported in Figure 1.

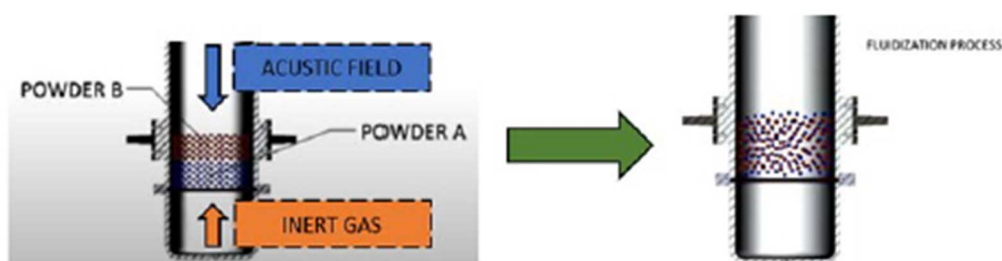


Fig. 1 – Scheme of POWMIX system, Sophia High Tech s.r.l. patent.

The powder object of this work, mixed by the POWMIX machine, consists of 65% copper and 35% 17-4 PH. The powder is then used to make specimens using the bed-fusion process in a Concept Laser M2 machine. The metal matrix composite was produce with the process parameters shown in Table 1. In particular, two print jobs were created corresponding to two sets of specimens to characterize the material with respect to both thermal and mechanical properties. The schematic design and the picture of the print jobs are shown in Figure 2. An insular randomic laser scanning strategy was used, which allows lower residual stresses [2] [3].

Table 1 – Process parameters.

Material	General	Body	Contour
Printing strategy	Island (lenght 5 mm)		
Layer thickness t [mm]	0.03		
Hatch distance h [mm]	0.105		
Spot size ϕ [mm]	0.15		
Speed v [mm/s]		253	400
Power P [W]	251		
Beam compensation δ [mm]			0.075
Overlap factor A1		0.7	

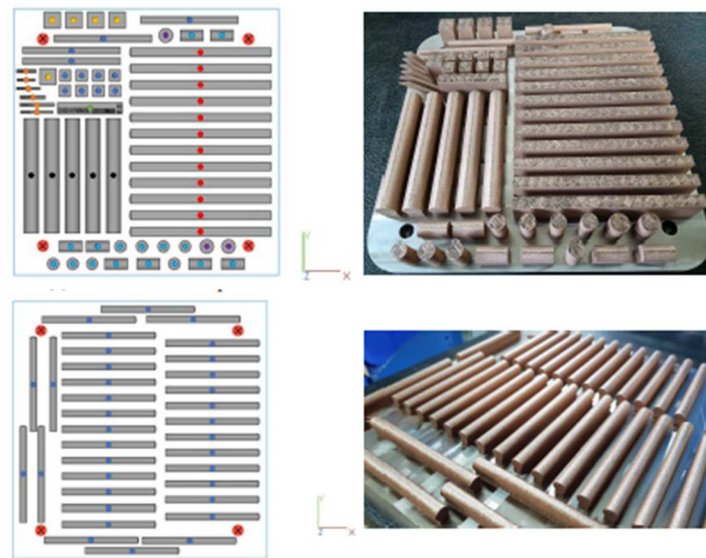


Fig. 2 – Job 1 (above) e Job 2 (below): design (left) and processing (right).

In the printing process, an XYZ reference system is defined in which the XY plane is the plane of the building platform and Z is the direction perpendicular to the plane, along which the product grows. For the mechanical characterization, 54 specimens were processed.

MICROGRAPHIC ANALYSIS

The microstructural observations were performed with a Keyence VHX microscope. An example of these observations is provided in Figure 3. The material obtained with the mixture selected for this research work (65% Cu - 35% 17-4PH) shows a composite microstructure with an interpenetrating bimetallic matrix, the two materials being insoluble. The composite is copper based and therefore it is possible to note that it constitutes the corresponding main matrix and the 17-4PH comes in island forms. Because copper has a lower melting point than 17-4PH, it melts well, insulating the steel. A possible hypothesis is that during the solidification process the copper, due to its greater thermal conductivity, solidifies before the 17-4PH, generating the base matrix. Subsequently the iron, which is 'floating' in the copper bath, solidifies with a more proper shape. This process makes this composite material complex. Another hypothesis to justify this structure envisages the phenomenon according to which copper has a greater capacity to flow in the liquid state because it lacks alloying elements and therefore slips into the gaps created by the iron which, being highly alloyed, flows more slowly. The microstructure observed in the XY plane (Figure 3) shows that the powder is homogeneously distributed along both the X and Y directions: the powder mixing process is able to obtain an excellent distribution of the components. The most interesting and innovative result that emerges from the micrographic analysis is that the material has two main regions that are fused independently and one well-mixed region (Figure 3):

- A copper matrix is clearly visible (orange region), and constitutes the main structure of the material;
- islands of 17-4PH are visible (blue regions);
- dotted matrix: this third group of areas consist of a high-density blend of copper and 17-4PH.

In the experiments reported in this work, the amount of energy absorbed by the powder bed below with a laser power equal to 251 [W] was insufficient to activate the keyhole phenomenon [4]. Generally, this phenomenon is more pronounced when a greater printing layer thickness is adopted because more material is processed in the same amount of time. Lower layer thickness values when powder mixtures are used as starting material may be investigated in future works.

In [5] and in [6] the micro-structure of a steel-copper samples produced by additive manufacturing is analyzed, showing that the transition zone is very similar to the microstructure observed in the present study. In particular, the authors find that depending on the copper concentration, multiple islands of different shapes with continuous interdendritic boundaries occur and the new composite material appears to have a qualitatively similar structure.

In the present research, the processed material does not show evident casting porosity and the layers arrangement seems to be affected by the composite components and distribution.

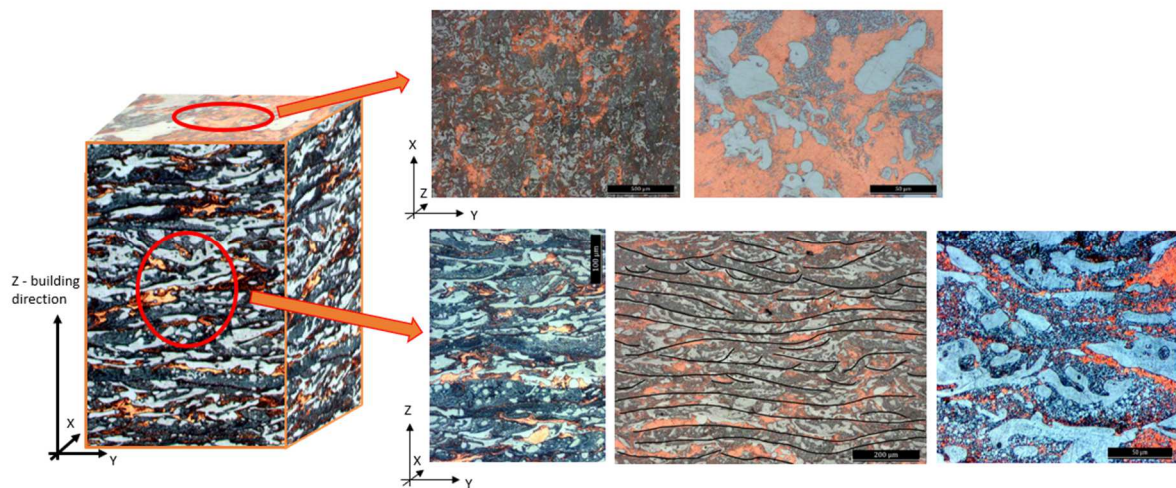


Fig. 3 – Micrographic images in XY (above) and Z (below) planes.

THERMAL PROPERTIES

To evaluate the thermal conductivity of Cu-17-4PH at room temperature, the “hot disk” method was employed using a dedicated instrument, the TPS1 2500. Disks were cut in different directions from the cylindrical and cubic specimens printed in Job1 (Figure 2). Both the 5 disks obtained from a cylinder specimen parallel to the XY plane and the 5 disks obtained from a cylinder specimen in the Z direction were subjected to measurement. Note that the thermal conductivity is measured with respect to the direction perpendicular to the section plane; thus, the XY section plane returns the conductivity in the Z direction and vice versa. The results of the thermal conductivity measurements for the new material are shown in Table 2.

Table 2. Thermal conductivity.

Plane	Thermal conductivity [W/mK]	Standard Deviation [W/mK]	% difference
XY	31.45	± 0.17	reference
Z	32.66	± 0.21	+3.8

The DSC (Differential Scanning Calorimetry) method was used to estimate the specific heat capacity of Cu-174PH using a Perkin-Elmer Pyris 1 Heat-Flux differential scanning calorimeter system. The test was performed in the temperature range from -40°C to 350°C. The specific heat capacity was calculated by applying the step isothermal temperature ramp. The result of the calorimetric measurement is shown in Figure 4, compared with the corresponding trends of the materials making up the composite.

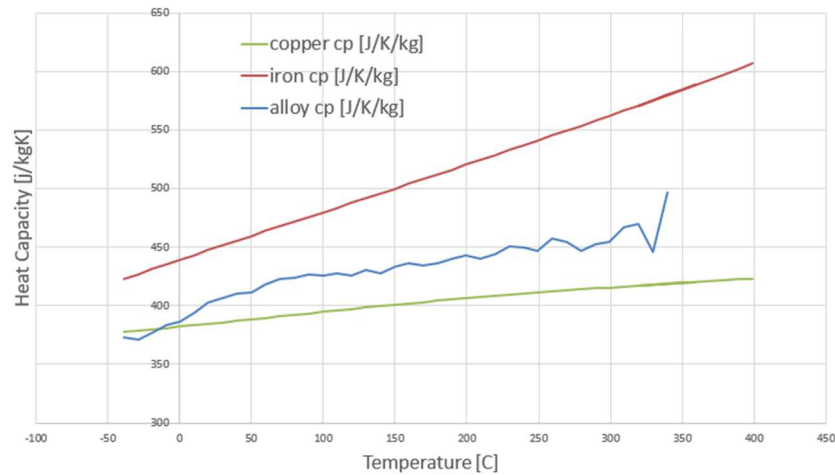


Fig. 4 – Composite Cu-174PH thermal capacity.

The TMA method (Thermomechanical Analysis) was employed to directly evaluate the coefficient of linear thermal expansion using a SETSYS Evolution Thermo Mechanical Analysis (TMA) system. Using the simple relationship $\Delta L = \alpha L_0 \Delta T$, where L_0 is the initial measurement length of the sample, ΔL is the length increase measured on the sample, and ΔT is the applied temperature increase, the expansion coefficient α is calculated for each temperature increment. The results of the measurements are shown in Figure 5. No time-dependent behavior of the coefficient was observed, as expected.

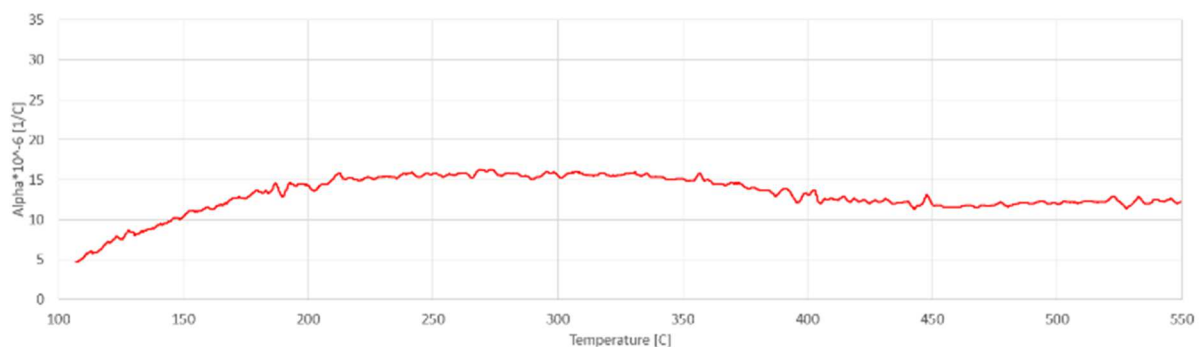


Fig. 5 – Cu-174PH linear thermal expansion coefficient.

MONOTONIC MECHANICAL PROPERTIES

To reduce the cost of the mechanical characterization, mainly driven by the cost of the powders, it was chosen to characterize only the tensile specimens with axis parallel to the XY plane. Therefore, the tensile test was performed with respect to the X or Y direction according to the

printing platform planar directions. The micrograph in Figure 6 represents the orientation of the microstructure of the tensile specimen. The tests were performed at room temperature, at 150°C, 350°C, 550°C and 650°C. For each temperature, 2 specimens were tested. The ambient temperature tests were performed on an Instron 8801 servo-hydraulic machine with a 100 kN load cell, while the tests at higher temperatures were performed on a Zwick Roell Z050 electromechanical machine with a 50 kN load cell. Both machines are located at the Polytechnic of Turin. The geometry of the specimens was created in accordance with ISO 6892, ASTM E8 and ASTM E21 standards.

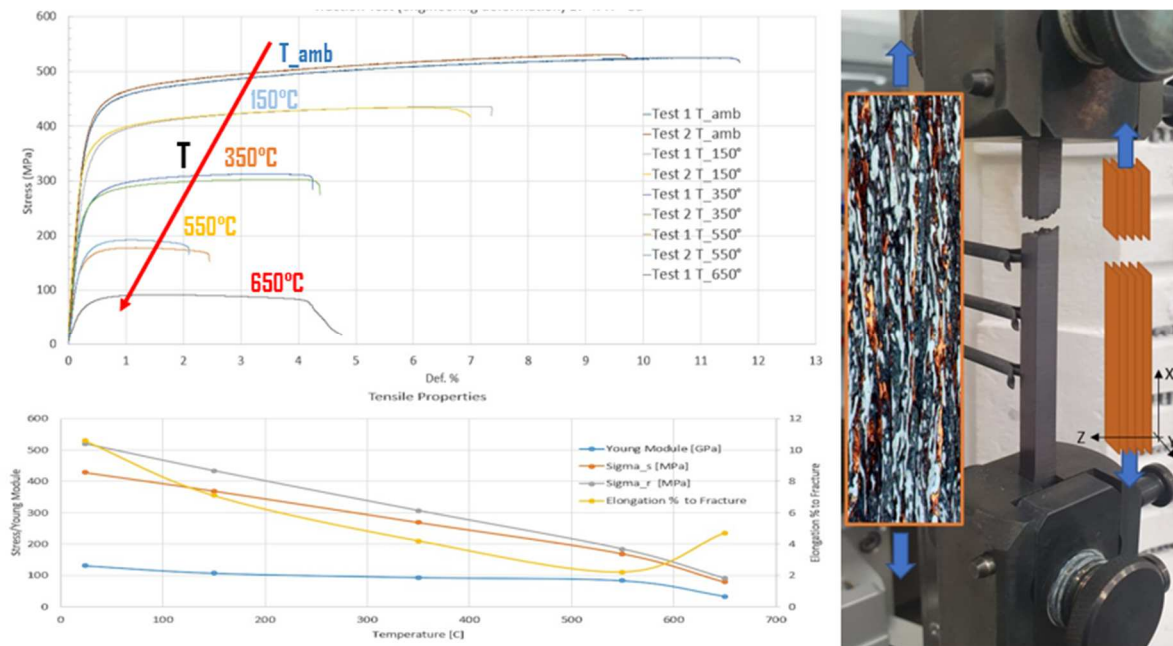


Fig. 6 – Room temperature and high temperature monotonic testing results.

The logic of the test campaign envisaged applying a temperature increase of 200°C, up to 550°C. Since the maximum temperatures foreseen in rocket engine application with copper-based materials is generally not much greater than 550°C, a further temperature step, 650°C, has been investigated in order to characterize the material behavior at the limit of its operative envelope. Analyzing the result at 650°C, the behavior of the material appears to be inelastic and therefore, not surprisingly, the limit for the stiff behavior of the Cu-174PH composite was set at a maximum reachable temperature of 550°C. The overall repeatability of tensile tests at different temperatures is very good. Interestingly, no pinching effects were observed. In fact, the slope of the tensile curve is positive for the entire test up to 550°C. This is probably mainly due to the inhomogeneity of the material.

The composite fracture mechanism shows a high temperature dependence, as reported in Figure 7 which compares fractures at room temperature and at 150°C. Compared to a common copper alloy, due to the low characteristic elongation of the tensile tests, it is possible to state that the material has a behavior comparable to a brittle composite. This is confirmed also for the case at 550°C, as can be observed in Figure 8. However, a more detailed surface fracture analysis shows locally 45° fracture surfaces. Therefore, the fracture mechanism is a hybrid between a ductile and a brittle behaviour.

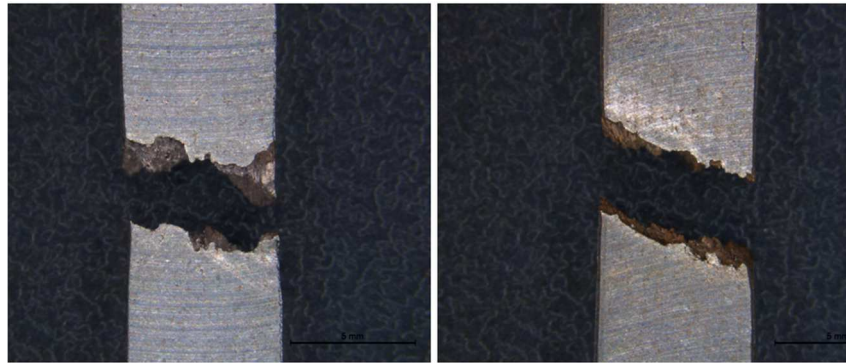


Fig. 7 – Monotonic failure profiles; room temperature (left) and 150°C (right).

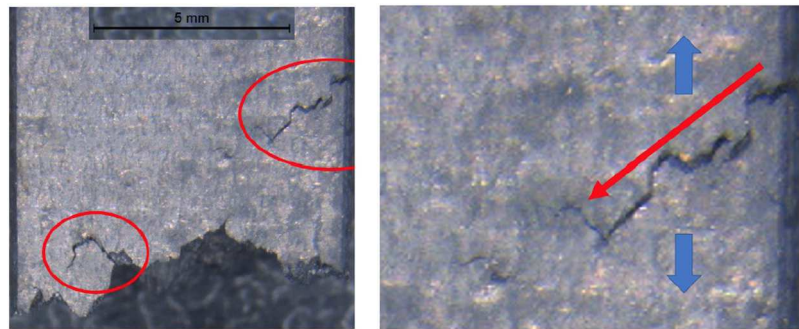


Fig. 8 – Monotonic failure profile; 550°C.

LOW CYCLE FATIGUE

The fatigue tests in the plastic field at room temperature were still performed on the Instron 8801 servohydraulic system of the Turin Polytechnic, while the tests at higher temperatures were performed at the CEROC of Tours with an INSTRON Electro-Thermal Mechanical Testing II system with 5 kN load. The geometry of the specimens was created in accordance with the ASTM E 606 and ISO 12106 standards. The total strain range intervals imposed were 0.5, 1.4, 2.0, 2.8, 3.6% for tests at room temperature, 2.0, 2.8, 3.6% for the tests at 150 and 350°C, and 1.0, 1.4, 2.0, 2.8, 3.6% for the tests at 550°C. Table 3 presents a summary of all results of low cycle fatigue. All tests were carried out with strain ratio $R=-1$ and up to failure of the specimen (except for two low strain tests at room temperature). The effect of mean stress or strain rate has not been investigated.

Figure 9 shows the stresses trends as the number of cycles varies. It is observed that apart from the typical oscillations of the single cycle, the stresses have an oscillating global trend, a trend that can be attributed to the presence of voids. In particular, when the local slope is positive the material is work hardening (the maximum stress increases with the cycles) and therefore the elastic modulus of the material is greater than the starting one: this is probably due to coalescence phenomena of the local voids. The more the voids collapse or combine, the less resistant area is available and therefore the material responds with a hardening behaviour. When, on the other hand, the local slope is negative, the material softens and the elastic modulus is reduced with respect to the previous maximum. In this phase, an increase in voids is observed. The porosities extend along the direction of traction without combining with each other: the local resistant area does not change and therefore, with the same deformation required, the material is able to deform better with less stress. After the local softening phase, it is possible to observe the flat section of the curve. However, after a few cycles, the voids (different shape, size and position) begin a new coalescence: this phenomenon is repetitive and local phenomena

of softening and hardening in the cycle can be observed in the experimental tests. This particular phenomenon, visible on the curve, can only be observed for low strains at room temperature. This could be due to the fact that, probably, there is a characteristic time to activate the phenomenon. If, on the other hand, we observe the tests carried out at higher temperatures and strain amplitudes, for example at 550°C and 1% strain amplitude, it is clearly visible (Figure 10) that the behavior is different from the tests at lower temperatures and an almost flat maximum/minimum stress trend can be observed. Figure 10 shows a particular random distribution of tensile and compressive stresses. In particular, there is local failure of the composite matrix which is probably caused by an instantaneous crack propagation which increases cycle after cycle. At the end of the void growth phase, the material begins to work harden until the final fracture is triggered.

Table 3 – LCF results.

	$\Delta \varepsilon_{eng. \%}$	Cycles to Fracture	$\varepsilon_{eng. \%}$		Stress eng. [MPa]		Stress [MPa] 50% cycles			Re-testing	
			Max	Min	Max	Min	Max	Min	Delta	Cycles to Fracture	Difference
T_amb	0.5	>6000	0.25	-0.25	200	-131	184	-94	278		
	1.4	>6000	0.71	-0.70	346	-279	318	-269	588		
	2.0	4180	1.01	-1.00	422	-393	382	-384	767		
	2.8	635	1.41	-1.40	487	-470	460	-469	930		
	3.6	136	1.81	-1.80	530	-529	517	-520	1037		
T_150	2.0	1447	1.01	-1.00	369	-335	338	-334	672		
	2.8	271	1.41	-1.40	418	-403	394	-392	787		
	3.6	63	1.80	-1.80	446	-440	429	-413	842		
T_350	2.0	795	1.00	-1.00	287	-350	280	-283	564		
	2.8	33	1.41	-1.40	352	-342	339	-338	677		
	3.6	14	1.80	-1.79	362	-364	354	-350	704		
T_550	1.0	1539	0.50	-0.50	162	-164	160	-156	316		
	1.4	546	0.70	-0.70	183	-187	178	-184	362	430	21.24%
	2.0	144	1.00	-1.00	203	-210	200	-207	407		
	2.8	39	1.40	-1.40	250	-255	247	-252	499	30	23.07%
	3.6	12	1.81	-1.80	232	-229	231	-228	459		

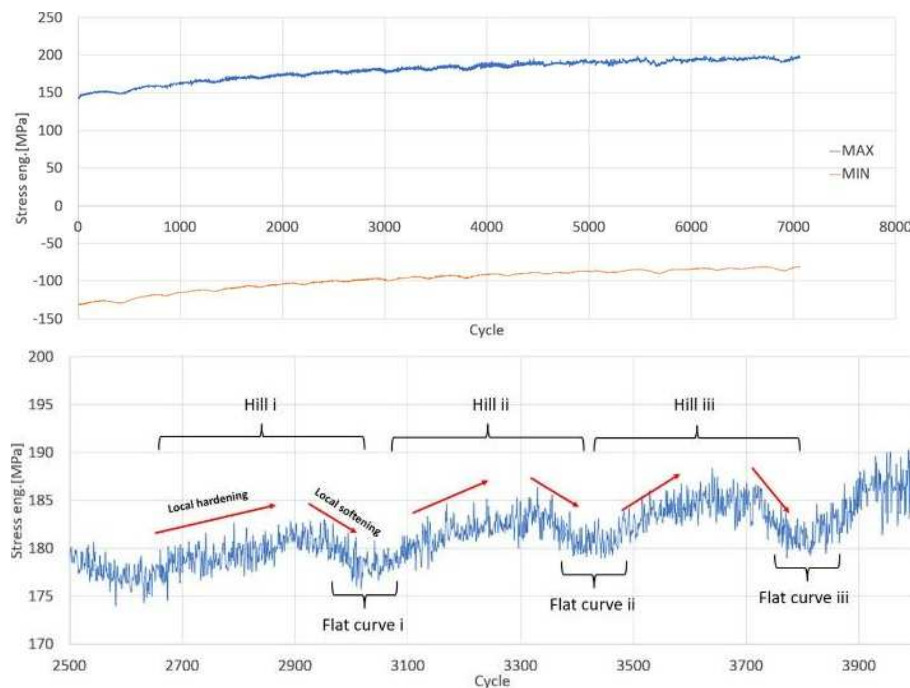


Fig. 9 – LCF room temperature. Stress trend for $\Delta \varepsilon=0.5\%$.

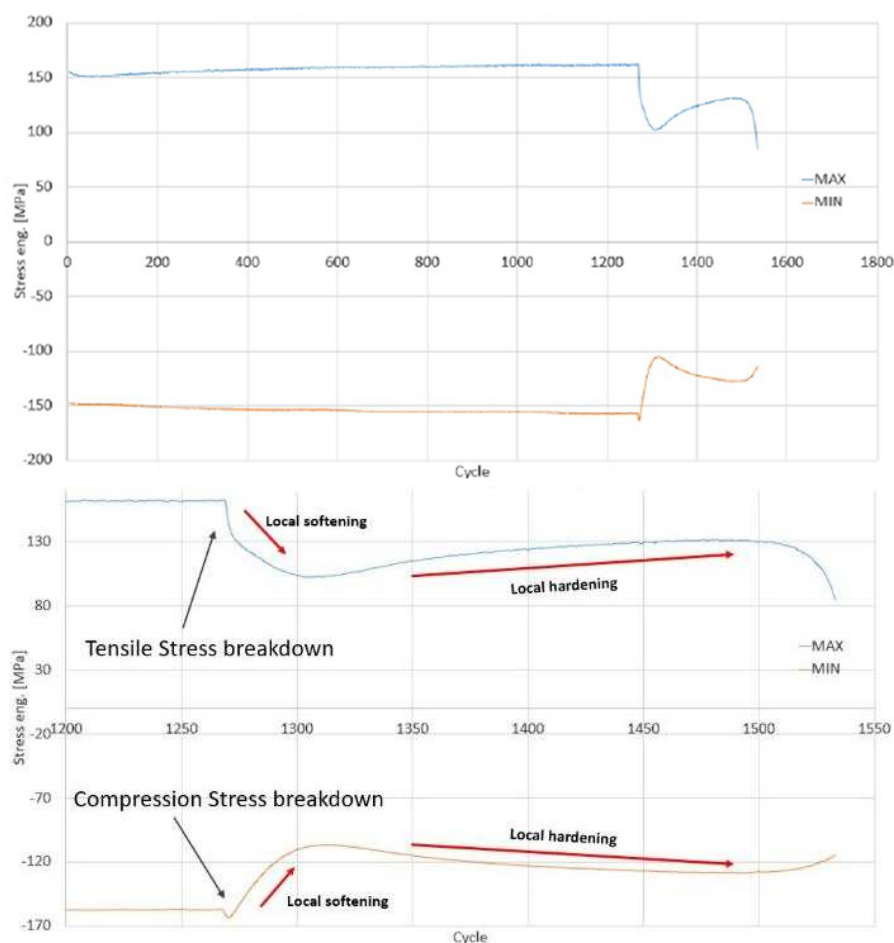


Fig. 10 – LCF 550°C. Stress trend for $\Delta\epsilon=1\%$.

CONCLUSIONS

The present work was developed to characterize the behavior of an innovative MMC (Metal Matrix Composite) tailored for additive manufacturing for space applications like liquid rocket engine thrust chambers.

In particular, the benefits brought by the mixing process of the powders before molding on the mechanical properties of the manufactured articles were investigated. The experimental campaign included static characterization, LCF at room temperature and at high temperature. The thermophysical properties were also characterized. Finally, the microstructure resulting from the additive printing process was studied.

The material was obtained by mixing two powders: 65% Cu and 35% 174PH. Micrographic analysis shows a bimetallic matrix composite microstructure. In particular, the main matrix is composed of copper with islands of 17-4PH. The microstructure is homogeneously distributed in the printing plane thanks to the mixing process of the powders. In the growth direction of the print the microstructure shows the melting pool phenomenon and not the keyhole; therefore, a better structure which still requires further optimization of the process parameters

The thermal conductivity does not show a relevant difference between the print plane and the perpendicular one. The specific heat capacity is a compromise between the two component materials. The coefficient of linear thermal expansion has a slight oscillation which could be

due to the particular bimetallic structure of the material, and to the additive manufacturing process.

Tensile properties exhibit very high tensile yield strength and very low elongation at fracture, especially at high temperatures. This is probably due to the different tensile behaviors of the component materials.

Fatigue tests at low number of cycles at room temperature and at high temperatures show a general slightly softening behavior, with the exception at 550°C.

REFERENCES

- [1] Di Veroli A, New space economy: (space 4.0). l'analisi dell'impatto socioeconomico delle attività spaziali nella promozione dello sviluppo dell'economia europea. 2021.
- [2] Salmi A, An integrated design methodology for components produced by laser powder bed fusion (l-pbf) process. 2018.
- [3] Harrison NJ, Reduction of micro-cracking in nickel superalloys processed by selective laser melting: A fundamental alloy design approach. *Acta Materialia*, 94, pp.59-68, 2015.
- [4] Svenungsson J, Choqueta I, Kaplan AFH, Laser welding process – a review of keyhole welding modelling, *Physics Procedia*, 78, pp.182-191 (2015).
- [5] Liu D, Thermo-structural analysis of regenerative cooling thrust chamber cylinder segment based on experimental data. *Chinese Journal of Aeronautics*, 33 (1), pp.102-115, 2020.
- [6] Osipovich S, Gradient transition zone structure in “steel–copper” sample produced by double wire-feed electron beam additive manufacturing. *Journal of material Science*, 55, pp.9258-9272, 2020.